


 Cite this: *RSC Adv.*, 2022, 12, 17846

# A fast-responsive fluorescent probe based on a styrylcoumarin dye for visualizing hydrogen sulfide in living MCF-7 cells and zebrafish†

 Xu Tong,<sup>a</sup> Liguao Hao,<sup>b</sup> Xue Song,<sup>a</sup> Shuang Wu,<sup>a</sup> Na Zhang,<sup>a</sup> Zhongtao Li,<sup>b</sup> Song Chen<sup>c</sup> and Peng Hou<sup>ib\*</sup>

As a vital antioxidant molecule, H<sub>2</sub>S can make an important contribution to regulating blood vessels and inhibiting apoptosis when present at an appropriate concentration. Higher levels of H<sub>2</sub>S can interfere with the physiological responses of the respiratory system and central nervous system carried out by mammalian cells. This is associated with many illnesses, such as diabetes, mental decline, cardiovascular diseases, and cancer. Therefore, the accurate measurement of H<sub>2</sub>S in organisms and the environment is of great significance for in-depth studies of the pathogenesis of related diseases. In this contribution, a new coumarin-carbazole-based fluorescent probe, COZ-DNBS, showing a rapid response and large Stokes shift was rationally devised and applied to effectively sense H<sub>2</sub>S *in vivo* and *in vitro*. Upon using the probe COZ-DNBS, the established fluorescent platform could detect H<sub>2</sub>S with excellent selectivity, showing 62-fold fluorescence enhancement, a fast-response time (<1 min), high sensitivity (38.6 nM), a large Stokes shift (173 nm), and bright-yellow emission. Importantly, the probe COZ-DNBS works well for monitoring levels of H<sub>2</sub>S in realistic samples, living MCF-7 cells, and zebrafish, showing that COZ-DNBS is a promising signaling tool for H<sub>2</sub>S detection in biosystems.

 Received 15th February 2022  
 Accepted 2nd June 2022

 DOI: 10.1039/d2ra00997h  
[rsc.li/rsc-advances](https://rsc.li/rsc-advances)

## 1. Introduction

In the process of maintaining biological homeostasis, reactive sulfur species (RSS), including hydrogen sulfide (H<sub>2</sub>S) and biological mercaptans (Cys, Hcy, and GSH), are essential thiol-containing molecules for resisting oxidative stress and maintaining the normal physiological function of organisms.<sup>1–3</sup> Numerous research works have revealed that H<sub>2</sub>S is considered to be a third endogenous gaseous transmitter after nitric oxide (NO) and carbon monoxide (CO).<sup>4–6</sup> As a vital antioxidant molecule, H<sub>2</sub>S can make an important contribution to the regulation of blood vessels and inhibition of apoptosis when present at an appropriate concentration.<sup>7–9</sup> Reports in the literature have suggested that the level of intracellular H<sub>2</sub>S can be significantly upregulated during inflammatory events. Higher levels of H<sub>2</sub>S can interfere with the physiological responses of the respiratory system and central nervous system carried out by mammalian cells. This is associated with many illnesses, such as diabetes, mental decline, cardiovascular diseases, and cancer.<sup>10–13</sup> Therefore, the accurate measurement of H<sub>2</sub>S in organisms and the

environment is of great significance for in-depth studies on the pathogenesis of related diseases.

Fluorogenic assays utilizing small-molecule fluorescent sensors have attracted wide attention in pharmacology and the life sciences because of the obvious advantages of non-invasive detection, excellent selectivity, rapid response, and the lack of need for pretreatment.<sup>14–18</sup> To date, numerous H<sub>2</sub>S-specific fluorescent probes have been established *via* exploiting various sensing mechanisms,<sup>19–24</sup> such as the thiolysis of 2,4-dinitrobenzenesulfonamide and dinitrophenyl ether groups; the reduction of azide, hydroxylamine, and nitro groups; nucleophilic addition with C=N<sup>+</sup> groups; and the high affinity of S<sup>2–</sup> for Cu<sup>2+</sup>. Although big breakthroughs have been made, some problems still need to be overcome, such as slow responses, small Stokes shifts (<100 nm), synthetic complexity, and low sensitivity, which have restricted the application of these sensors in the fields of biochemistry and biomedicine. A fluorescent probe with a large Stokes shift is more preferred because it is relatively easy to reduce self-quenching and auto-fluorescence during fluorescence sensing.<sup>25–27</sup> This method can remarkably improve the detection accuracy. Moreover, a rapid response is an important index for optical sensors used for the real-time monitoring and bio-imaging of H<sub>2</sub>S in biological systems. Thus, the development of a H<sub>2</sub>S-specific fluorescent probe with excellent properties is particularly necessary.

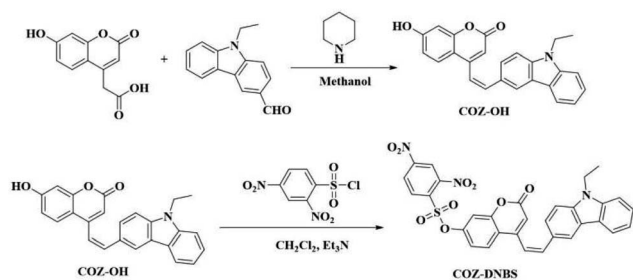
Combining all these considerations, in this work, a new coumarin-carbazole-based fluorescent probe, COZ-DNBS, with

<sup>a</sup>The Third Affiliated Hospital, Qiqihar Medical University, Qiqihar 161006, China

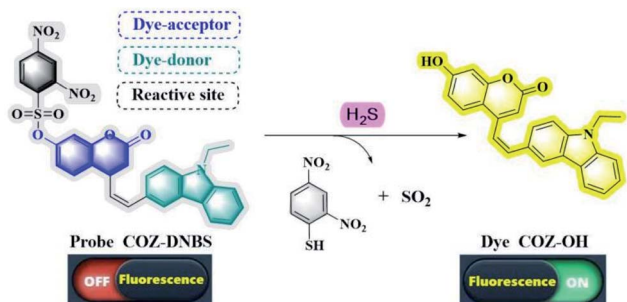
<sup>b</sup>College of Medical Technology, Qiqihar Medical University, Qiqihar 161006, China

<sup>c</sup>College of Pharmacy, Qiqihar Medical University, Qiqihar 161006, China. E-mail: [houpeng1982@163.com](mailto:houpeng1982@163.com)

 † Electronic supplementary information (ESI) available. See <https://doi.org/10.1039/d2ra00997h>

Scheme 1 The synthetic route to the new fluorescent probe COZ-DNBS.



Scheme 2 The proposed mechanism involving the fluorescent probe COZ-DNBS for H<sub>2</sub>S detection.

a rapid response and large Stokes shift was rationally devised and applied to effectively sense H<sub>2</sub>S *in vivo* and *in vitro*. The concrete synthesis route for COZ-DNBS is depicted in Scheme 1, and the structures of COZ-OH and COZ-DNBS were characterized *via* HRMS and <sup>13</sup>C-NMR and <sup>1</sup>H-NMR spectroscopy (Fig. S2–S7†). Structurally, in order to lengthen the emission wavelength, a carbazole group was modified onto the coumarin core to extend the  $\pi$ -conjugation structure. 2,4-Dinitrobenzenesulfonyl (DNBS), an outstanding fluorescence quenching moiety, served as the reactive site for H<sub>2</sub>S,<sup>28,29</sup> while the newly synthesized coumarin-carbazole dye COZ-OH was employed as the fluorophore (Scheme 2). When using the probe COZ-DNBS, the established fluorescent platform could detect H<sub>2</sub>S with excellent selectivity, showing 62-fold fluorescence enhancement, a fast response (<1 min), high sensitivity (38.6 nM), a large Stokes shift (173 nm), and bright-yellow emission (Table S1†). Importantly, the probe COZ-DNBS works well when monitoring levels of H<sub>2</sub>S in realistic samples, living MCF-7 cells, and zebrafish, showing that COZ-DNBS is a promising signaling tool for H<sub>2</sub>S detection in biosystems.

## 2. Experimental

### 2.1 Instruments and reagents

HRMS (high-resolution mass spectroscopy) analysis was carried out using AB Sciex TripleTOF 4600 apparatus. <sup>1</sup>H- and <sup>13</sup>C-NMR (nuclear magnetic resonance) spectra were obtained using a Bruker Avance 600 MHz spectrometer. The UV-vis absorption and fluorescence spectra data were obtained using a Shimadzu

UV-2450 spectrometer and HITACHI F-4600 fluorescence spectrophotometer. Fluorescence images of cells and zebrafish were acquired using a Zeiss LSM710 Wetzlar laser scanning confocal microscope. All chemicals were purchased from suppliers in China and used directly without further refining.

### 2.2 Synthesis of the dye COZ-OH

7-Hydroxycoumarin-4-acetic acid (110.0 mg, 0.5 mmol) and *N*-ethylcarbazole-3-carbaldehyde (116.4 mg, 0.5 mmol) were dissolved in 6.0 mL of CH<sub>3</sub>OH, and then piperidine (46.0  $\mu$ L) was added to the above mixed solution. After stirring for 12.0 h at 75 °C, the reaction was completed. The cooled precipitate was washed with cold methanol (10.0 mL), whereafter the obtained solid was extracted using dichloromethane/brine (15.0 mL/50.0 mL) and dried over Na<sub>2</sub>SO<sub>4</sub>. The crude product was purified *via* column chromatography (CH<sub>2</sub>Cl<sub>2</sub> : CH<sub>3</sub>OH = 50 : 1) to give the dye COZ-OH (97.2 mg, 51% yield). <sup>1</sup>H NMR (600 MHz, DMSO)  $\delta$  (ppm) 10.58 (s, 1H), 8.67 (s, 1H), 8.18 (dd,  $J$  = 41.8, 8.2 Hz, 2H), 7.96–7.63 (m, 5H), 7.50 (t,  $J$  = 7.6 Hz, 1H), 7.27 (t,  $J$  = 7.4 Hz, 1H), 6.87 (dd,  $J$  = 8.7, 1.8 Hz, 1H), 6.77 (d,  $J$  = 1.8 Hz, 1H), 6.58 (s, 1H), 4.48 (q,  $J$  = 7.0 Hz, 2H), 1.34 (t,  $J$  = 7.1 Hz, 3H). <sup>13</sup>C NMR (151 MHz, DMSO)  $\delta$  (ppm) 161.69, 161.34, 155.89, 151.00, 140.84, 140.57, 139.48, 127.45, 127.15, 126.90, 126.67, 123.10, 122.75, 120.97, 120.89, 119.81, 117.19, 113.27, 111.33, 110.01, 109.90, 103.88, 103.05, 37.63, 14.23. HRMS (ESI)  $m/z$ : calcd for [C<sub>25</sub>H<sub>20</sub>NO<sub>3</sub>]<sup>+</sup>, 382.1443; found, 382.1422.

### 2.3 Synthesis of the probe COZ-DNBS

COZ-OH (38.0 mg, 0.1 mmol) and 30.0  $\mu$ L of Et<sub>3</sub>N were mixed in 8.0 mL of CH<sub>2</sub>Cl<sub>2</sub> at room temperature for 10.0 min. Then, 2,4-dinitrobenzenesulfonyl chloride (32.0 mg, 0.12 mmol) was added into the mixture and it was stirred for 6.5 h. After natural cooling, the reaction solution was filtered and dried over Na<sub>2</sub>SO<sub>4</sub>. The crude product was purified *via* silica gel column chromatography using CH<sub>2</sub>Cl<sub>2</sub> as the eluent to obtain COZ-DNBS (47.1 mg, 77% yield). <sup>1</sup>H NMR (600 MHz, DMSO)  $\delta$  (ppm) 9.14 (d,  $J$  = 2.3 Hz, 1H), 8.66 (s, 1H), 8.62 (dd,  $J$  = 8.7, 2.3 Hz, 1H), 8.42 (d,  $J$  = 8.9 Hz, 1H), 8.35 (d,  $J$  = 8.7 Hz, 1H), 8.19 (d,  $J$  = 7.7 Hz, 1H), 7.99–7.89 (m, 2H), 7.73–7.63 (m, 3H), 7.54–7.47 (m, 1H), 7.40 (d,  $J$  = 2.4 Hz, 1H), 7.30–7.24 (m, 2H), 6.89 (s, 1H), 4.49 (d,  $J$  = 7.2 Hz, 2H), 1.34 (t,  $J$  = 7.1 Hz, 3H). <sup>13</sup>C NMR (151 MHz, DMSO)  $\delta$  (ppm) 160.22, 154.56, 152.11, 150.53, 149.94, 148.63, 140.99, 140.63, 140.58, 134.19, 131.01, 128.12, 127.97, 127.29, 126.98, 126.74, 123.08, 122.71, 121.72, 121.18, 120.90, 119.90, 118.98, 118.37, 116.34, 111.27, 110.08, 109.98, 108.31, 37.65, 14.24. HRMS (ESI)  $m/z$ : calcd for [C<sub>31</sub>H<sub>22</sub>N<sub>3</sub>O<sub>9</sub>S]<sup>+</sup>, 612.1077; found, 612.1074.

### 2.4 Procedure for optical data measurements

COZ-DNBS was dissolved using CH<sub>3</sub>CN and a stock solution was prepared with a concentration of 3.0 mM. 10.0 mM analyte stock solutions (including Ala, Asn, Arg, Glu, Gln, Met, Ser, His, Pro, Thr, Ile, Cys, GSH, Hcy, Cl<sup>-</sup>, Br<sup>-</sup>, F<sup>-</sup>, I<sup>-</sup>, NO<sub>3</sub><sup>-</sup>, CO<sub>3</sub><sup>2-</sup>, SO<sub>4</sub><sup>2-</sup>, Zn<sup>2+</sup>, H<sub>2</sub>O<sub>2</sub>, and NaHS) were made up in deionized water for immediate use. All solution tests were performed in pH 7.4 PBS/CH<sub>3</sub>CN (4 : 1, v/v). The fluorescence spectra were obtained

at  $\lambda_{\text{ex}} = 400.0$  nm. **COZ-DNBS** was dissolved in DMSO for cell culture and zebrafish studies.

## 2.5 Cell cultures and imaging

Human breast carcinoma MCF-7 cells were plated in a confocal Petri dish with DMEM culture medium to adherence for 24 h. As a control, MCF-7 cells were immersed in  $10.0 \mu\text{M}$  **COZ-DNBS** at  $37^\circ\text{C}$  for 30 min. For the experiment groups, MCF-7 cells were pre-incubated with different concentrations of  $\text{H}_2\text{S}$  ( $10.0$ ,  $20.0$ , and  $50.0 \mu\text{M}$ , respectively) for 30 min and further treated with **COZ-DNBS** ( $10.0 \mu\text{M}$ ) for another 30 min. After rinsing the confocal Petri dish with phosphate-buffered saline (PBS) three times to remove residue, the MCF-7 cells were imaged using a Zeiss LSM 710 laser scanning confocal microscope.

## 2.6 Zebrafish imaging

Four-day-old zebrafish were obtained from Eze-Rinka Company (Nanjing, China). Firstly, the zebrafish to be imaged were incubated with the probe **COZ-DNBS** ( $10.0 \mu\text{M}$ ) at  $37^\circ\text{C}$  for 30 min, and they were then imaged following three cycles of PBS washing. Subsequently, other zebrafish were pretreated with  $50.0 \mu\text{M}$   $\text{H}_2\text{S}$  for 30 min and stained with **COZ-DNBS** ( $10.0 \mu\text{M}$ ) for another 30 min. After washing with PBS three times, fluorescence imaging was performed using a confocal microscope.

## 2.7 Preparation of spiked samples

The river water, lake water, and tap water samples used in these experiments were obtained from the Nenjiang river, Laodong lake, and a laboratory in Qiqihar Medical University, respectively. After being filtered, the above real water samples were spiked with different concentrations of  $\text{H}_2\text{S}$  ( $5.0$ ,  $10.0$ , and  $20.0 \mu\text{M}$ ), and then the fluorescence intensity changes of the mixtures were measured in triplicate.

# 3. Results and discussion

## 3.1 Spectral response

To understand the optical properties of **COZ-DNBS** when it reacted with  $\text{H}_2\text{S}$ , fluorescence titration was carried out in pH 7.4 PBS/ $\text{CH}_3\text{CN}$  (4 : 1, v/v) with various concentrations of  $\text{H}_2\text{S}$  (Fig. 1). It was seen that the photoinduced electron transfer (PET)-based emission of **COZ-DNBS** resulted in “turn-off” fluorescence being observed in the absence of  $\text{H}_2\text{S}$ . Upon the addition of  $\text{H}_2\text{S}$ , **COZ-DNBS** showed dramatic fluorescence emission centered at  $558$  nm and with a large Stokes shift ( $173$  nm) (Fig. S1†). With an increase in the  $\text{H}_2\text{S}$  concentration, the fluorescence enhanced gradually and showed a 62-fold increase upon the addition of  $60.0 \mu\text{M}$   $\text{H}_2\text{S}$ . Based on previous research,<sup>30,31</sup> the above profound optical changes at  $558$  nm for **COZ-DNBS** in the presence of  $\text{H}_2\text{S}$  should be ascribed to the formation of the dye **COZ-OH**. This sensing strategy was also verified based on the HRMS spectra. A mixture of **COZ-DNBS** and  $\text{H}_2\text{S}$  (cal.:  $382.1415$ ) (Fig. S8†) has nearly the same molecular weight as **COZ-OH** ( $m/z = 382.1443$ ) (Fig. S6†). Moreover, the regression equation was obtained according to the dose-dependent spectral response, and it displayed a good linear

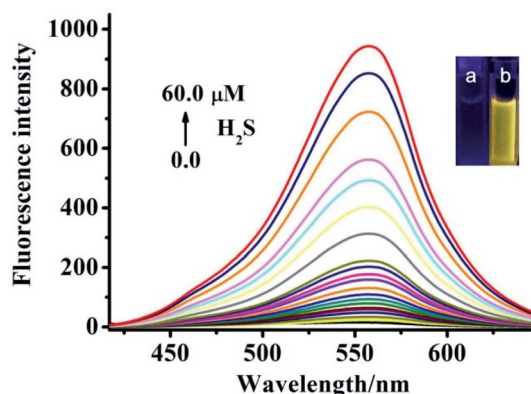


Fig. 1 Fluorescence spectra of **COZ-DNBS** ( $10.0 \mu\text{M}$ ) in the presence of different amounts of  $\text{H}_2\text{S}$  ( $0.0$ – $60.0 \mu\text{M}$ ); inset: the colorimetric changes of **COZ-DNBS** without (a) and with (b)  $\text{H}_2\text{S}$ .

relationship between the fluorescence intensity and concentration of  $\text{H}_2\text{S}$  (Fig. 2). In the concentration range of  $0.0$ – $5.0 \mu\text{M}$ , the limit of detection (LOD) for  $10.0 \mu\text{M}$  **COZ-DNBS** was estimated to be  $38.6$  nM, suggesting that the probe **COZ-DNBS** had the potential to detect  $\text{H}_2\text{S}$  qualitatively and quantitatively.

## 3.2 Selectivity study

To prove the sensitivity and specificity of **COZ-DNBS** for identifying  $\text{H}_2\text{S}$ , a series of analytes was employed and monitored in aqueous media. As depicted in Fig. 3, the fluorescence intensity of **COZ-DNBS** hardly changed upon adding various amino acids, ions, and biologically active materials (including Ala, Asn, Arg, Glu, Gln, Met, Ser, His, Pro, Thr, Ile,  $\text{Cl}^-$ ,  $\text{Br}^-$ ,  $\text{F}^-$ ,  $\text{I}^-$ ,  $\text{NO}_3^-$ ,  $\text{CO}_3^{2-}$ ,  $\text{SO}_4^{2-}$ ,  $\text{Zn}^{2+}$ ,  $\text{H}_2\text{O}_2$ , Cys, GSH, and Hcy). However, a remarkable fluorescence response with an approximately 62-fold enhancement ratio at  $558$  nm was seen in the presence of  $\text{H}_2\text{S}$  compared with the slight fluorescence behavior induced by biothiols (Cys, Hcy and GSH), which indicated that **COZ-DNBS** had good sensing abilities towards  $\text{H}_2\text{S}$ . In addition, competition experiments, involving the coexistence of the

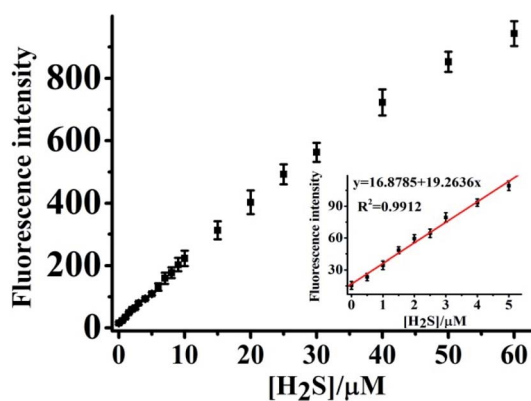


Fig. 2 The fluorescence intensity of **COZ-DNBS** at  $558$  nm as a function of the  $\text{H}_2\text{S}$  dose ( $0.0$ – $60.0 \mu\text{M}$ ); inset: the linear relationship between the concentration of  $\text{H}_2\text{S}$  ( $0.0$ – $5.0 \mu\text{M}$ ) and the fluorescence intensity at  $558$  nm.

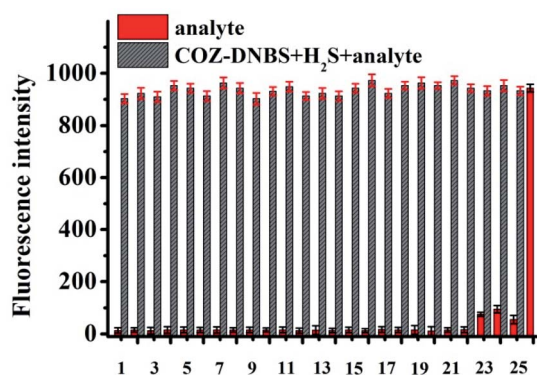


Fig. 3 The fluorescence responses of COZ-DNBS (10.0 μM) incubated with various analytes (red bars; 60.0 μM for H<sub>2</sub>S (26) and 0.5 mM for 1–25, which were Ala, Asn, Arg, Glu, Gln, Met, Ser, His, Pro, Thr, Ile, Cl<sup>-</sup>, Br<sup>-</sup>, F<sup>-</sup>, I<sup>-</sup>, NO<sub>3</sub><sup>-</sup>, CO<sub>3</sub><sup>2-</sup>, SO<sub>4</sub><sup>2-</sup>, Zn<sup>2+</sup>, H<sub>2</sub>O<sub>2</sub>, Cys, GSH, and Hcy, respectively); and the detection of H<sub>2</sub>S (60.0 μM) upon the addition of diverse coexisting competing analytes (gray bars; 0.5 mM for Ala, Asn, Arg, Glu, Gln, Met, Ser, His, Pro, Thr, Ile, Cl<sup>-</sup>, Br<sup>-</sup>, F<sup>-</sup>, I<sup>-</sup>, NO<sub>3</sub><sup>-</sup>, CO<sub>3</sub><sup>2-</sup>, SO<sub>4</sub><sup>2-</sup>, Zn<sup>2+</sup>, H<sub>2</sub>O<sub>2</sub>, Cys, GSH, and Hcy (1–25, respectively)). The incubation time was 60 s.

aforementioned analytes (including Ala, Asn, Arg, Glu, Gln, Met, Ser, His, Pro, Thr, Ile, Cl<sup>-</sup>, Br<sup>-</sup>, F<sup>-</sup>, I<sup>-</sup>, NO<sub>3</sub><sup>-</sup>, CO<sub>3</sub><sup>2-</sup>, SO<sub>4</sub><sup>2-</sup>, Zn<sup>2+</sup>, H<sub>2</sub>O<sub>2</sub>, Cys, GSH, and Hcy), were performed to explore the feasibility of using COZ-DNBS to detect H<sub>2</sub>S. It is found that the degree of fluorescence intensity change was similar as that in the presence of H<sub>2</sub>S alone, demonstrating that COZ-DNBS could selectively respond to H<sub>2</sub>S in complex biological environments.

### 3.3 Kinetics and pH studies

To obtain the optimal fluorescence sensing set-up for H<sub>2</sub>S detection, it is important to optimize the pH to obtain the highest response of COZ-DNBS towards H<sub>2</sub>S. In the present study, the effects of pH were explored in the range of pH 2 to 11. As shown in Fig. 4, the free probe COZ-DNBS exhibited a very weak emissive nature at 558 nm in diverse pH environments. After the addition of H<sub>2</sub>S, the fluorescence intensity of COZ-

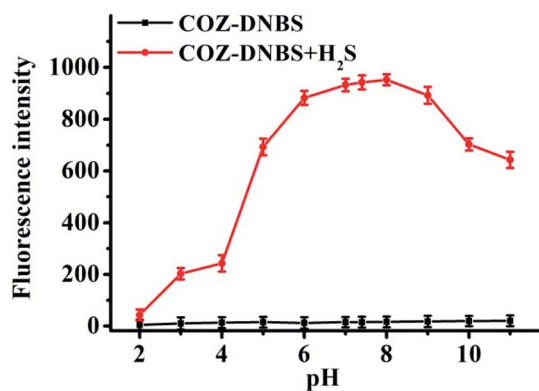


Fig. 4 The pH-dependence (2.0–11.0) of the fluorescence intensity of COZ-DNBS (10.0 μM) in H<sub>2</sub>O/CH<sub>3</sub>CN (4 : 1, v/v) without (black line) and with (red line) H<sub>2</sub>S (60.0 μM).

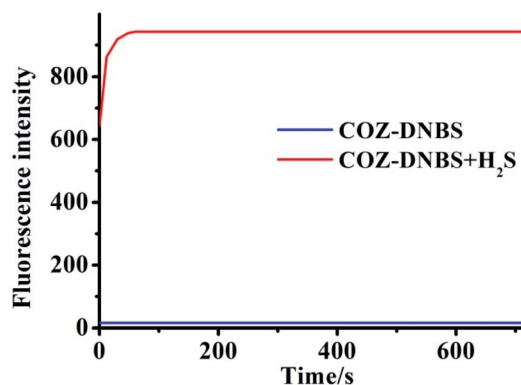


Fig. 5 The fluorescence intensity of COZ-DNBS (10.0 μM) over time at 558 nm before (blue line) and after (red line) the addition of H<sub>2</sub>S.

DNBS increased gradually from pH 2.0 to 5.0; a high fluorescence signal value emerged between 6.0 and 8.0, and this slightly decreased under alkaline conditions. The above results strengthen the possibility of using COZ-DNBS as a candidate probe for H<sub>2</sub>S detection under neutral conditions. Subsequently, the time-dependent fluorescence changes of COZ-DNBS in the presence of H<sub>2</sub>S were studied (Fig. 5). In the pH 7.4 PBS/CH<sub>3</sub>CN (4 : 1, v/v) system, the observed fluorescence intensity of COZ-DNBS alone remained unchanged, meaning that COZ-DNBS possessed excellent stability in the liquid state. However, the fluorescence signal of COZ-DNBS immediately increased (in less than 1 min) in this buffer system after adding H<sub>2</sub>S, and the bright fluorescence of the reaction product between COZ-DNBS and H<sub>2</sub>S was insensitive to the incubation time. This clearly indicates that COZ-DNBS has the real-time capability to detect H<sub>2</sub>S.

### 3.4 Imaging of H<sub>2</sub>S in living MCF-7 cells

Prompted by the favorable properties of COZ-DNBS, the bio-imaging abilities of COZ-DNBS were studied *via* living cell analysis. Before intracellular imaging, the cytotoxicity of COZ-DNBS toward MCF-7 cells was assessed *via* MTT assays. The results showed that COZ-DNBS displayed low cytotoxicity in the

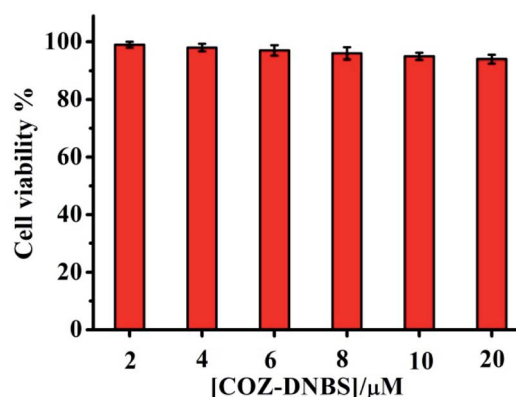


Fig. 6 The viability of MCF-7 cells incubated with different concentrations of COZ-DNBS (2.0–20.0 μM).

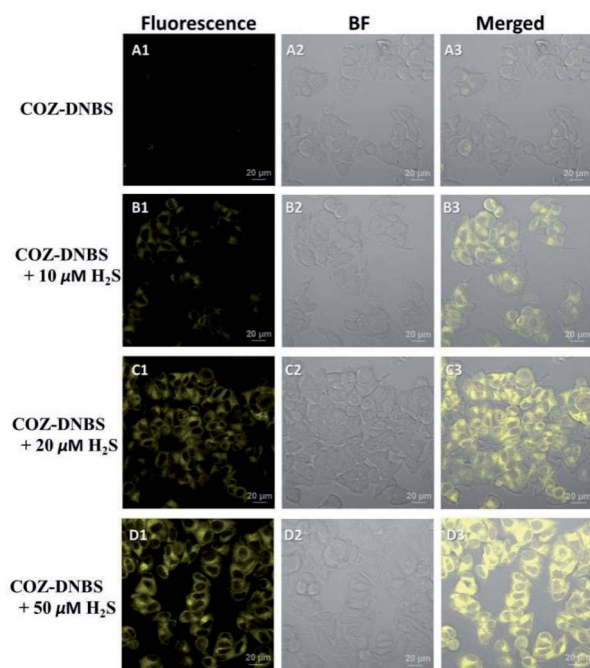


Fig. 7 Confocal imaging of MCF-7 cells: (A) MCF-7 cells incubated with 10.0 μM COZ-DNBS for 30 min; and (B–D) MCF-7 cells incubated with different concentrations of H<sub>2</sub>S (10.0, 20.0, and 50.0 μM), followed by treatment with 10.0 μM COZ-DNBS.

range of 2–20.0 μM, with above 94% cell viability (Fig. 6), indicating that COZ-DNBS was biocompatible for performing imaging in living organisms. Subsequently, the probe COZ-DNBS was applied to monitor intracellular H<sub>2</sub>S in MCF-7 cells. As shown in Fig. 7, a slight fluorescence background signal emerged when MCF-7 cells were treated with COZ-DNBS alone, which may arise from the presence of a very small amount of H<sub>2</sub>S in the cells. However, the appearance of remarkable fluorescence was observed in the presence of H<sub>2</sub>S (Fig. 7B1–D1), and the fluorescence signal increased gradually with an increase (10.0–50.0 μM) in the H<sub>2</sub>S concentration. The above findings demonstrated that COZ-DNBS could be used to quantify the concentration of H<sub>2</sub>S based on the relative fluorescence intensity from images of live cells.

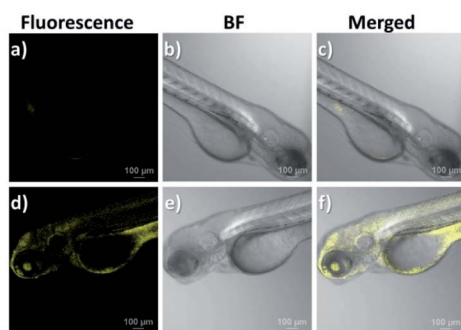


Fig. 8 Fluorescence imaging of H<sub>2</sub>S in zebrafish using COZ-DNBS: (a–c) zebrafish incubated with COZ-DNBS (10.0 μM) for 30 min; and (d–f) zebrafish incubated with H<sub>2</sub>S (50.0 μM) before staining with COZ-DNBS (10.0 μM).

### 3.5 Imaging of H<sub>2</sub>S in living zebrafish

The potential application of imaging H<sub>2</sub>S in living zebrafish upon incubation with COZ-DNBS was then validated. As depicted in Fig. 8, incubation with COZ-DNBS (10.0 μM) led to only a weak fluorescence signal from H<sub>2</sub>S already present in the zebrafish in the yellow channel. In contrast, the fluorescence signal became much brighter after the addition of H<sub>2</sub>S (50.0 μM). It was advantageously confirmed that COZ-DNBS could be suitable for the detection of H<sub>2</sub>S in living zebrafish, showing excellent membrane permeability.

### 3.6 Detection of H<sub>2</sub>S in spiked samples

To further gauge the feasibility of using the probe COZ-DNBS for practical applications, the quantitative analysis of real samples was investigated. In three different water samples (river water, lake water, and tap water), spiked H<sub>2</sub>S concentrations were measured using COZ-DNBS. As manifested *via* recovery experiments (Table S2<sup>†</sup>), moderate to good recovery rates were obtained when using COZ-DNBS to sensitively detect H<sub>2</sub>S, within the range of 95.6–103.4%, and the relative standard deviation (RSD) values were less than 3.0%. The above data showed that the proposed COZ-DNBS sensor exhibited excellent accuracy in actual water samples, proving the capacity of COZ-DNBS to act as a valid tool for the detection of H<sub>2</sub>S in environmental samples.

## 4. Conclusions

In conclusion, we have achieved a new fluorescent probe, COZ-DNBS, for H<sub>2</sub>S detection based on the novel coumarin-carbazole fluorescent dye COZ-OH. Upon reaction with H<sub>2</sub>S, COZ-DNBS exhibited high sensitivity (38.6 nM), excellent selectivity, and extraordinary fluorescence enhancement (62-fold) in the yellow region ( $\lambda_{\text{maxem}} = 558 \text{ nm}$ ). Moreover, benefiting from the fast response (<1 min) and huge Stokes shift (173 nm), COZ-DNBS was successfully applied to the detection of H<sub>2</sub>S in realistic samples, living MCF-7 cells, and zebrafish, and it displayed great potential for H<sub>2</sub>S detection in biosystems.

## Ethical statement

All animal procedures were performed in accordance with the Guidelines for the Care and Use of Laboratory Animals of Qiqihar Medical University and experiments were approved by the Animal Ethics Committee of Qiqihar Medical University (QMU-AECC-2020-63).

## Conflicts of interest

There are no conflicts of interest to declare.

## Acknowledgements

Thanks is extended for the financial support provided by the Clinical research fund project of Qiqihar Academy of Medical Sciences (No. QMSI2021L-21).

## References

- 1 Y. F. Rong, P. X. Niu, X. J. Liu, W. Q. Chen, L. H. Wei and X. Z. Song, Double-channel based fluorescent probe for differentiating GSH and H<sub>2</sub>Sn ( $n > 1$ ) via a single-wavelength excitation with long-wavelength emission, *Sens. Actuators, B*, 2021, **344**, 130224.
- 2 Y. Y. Li, G. X. Zhang, C. J. Ma, F. H. Chen, J. Dong and Y. Q. Ge, A simple dual-channel imidazo[1,5- $\alpha$ ]pyridine-based fluorescent probe for the discrimination between Cys/Hcy and GSH, *Dyes Pigm.*, 2021, **191**, 109381.
- 3 J. Zhang, G. H. Wen, W. H. Wang, K. Cheng, Q. Guo, S. Tian, C. Liu, H. R. Hu, Y. C. Zhang, H. T. Zhang, L. D. Wang and H. Y. Sun, Controllable cleavage of C–N bond-based fluorescent and photoacoustic dual-modal probes for the detection of H<sub>2</sub>S in living mice, *ACS Appl. Bio Mater.*, 2021, **4**, 2020–2025.
- 4 Y. Sun, C. Li, X. W. Feng, C. F. Wang, N. Wang, J. R. Zhu, T. Wang and X. Y. Cui, Si-coumarin-based fluorescent probes for ultrafast monitoring H<sub>2</sub>S *in vivo*, *Dyes Pigm.*, 2021, **186**, 109059.
- 5 B. B. Wang, X. Q. Wang, A. Q. Zeng, J. C. Leng and W. Zhao, Engineering a mitochondria-targeted ratiometric fluorescent probe with a large stokes shift for H<sub>2</sub>S-specific assaying in foodstuffs and living cells, *Sens. Actuators, B*, 2021, **343**, 130095.
- 6 K. Q. Zhang, J. Q. Meng, W. E. Bao, M. Liu, X. F. Wang and Z. Y. Tian, Mitochondrion-targeting near-infrared fluorescent probe for detecting intracellular nanomolar level hydrogen sulfide with high recognition rate, *Anal. Bioanal. Chem.*, 2021, **413**, 1215–1224.
- 7 Y. L. Zheng, Z. H. Chai, W. Tang, S. Yan, F. Dai and B. Zhou, A multi-signal mitochondria-targetable fluorescent probe for simultaneously discriminating Cys/Hcy/H<sub>2</sub>S, GSH, and SO<sub>2</sub> and visualizing the endogenous generation of SO<sub>2</sub> in living cells, *Sens. Actuators, B*, 2021, **330**, 129343.
- 8 K. L. Zhong, X. L. Hu, S. Y. Zhou, X. Y. Liu, X. Gao, L. J. Tang and X. M. Yan, Mitochondria-targeted red-emission fluorescent probe for ultrafast detection of H<sub>2</sub>S in food and its bioimaging application, *J. Agric. Food Chem.*, 2021, **69**, 4628–4634.
- 9 L. Zhou, Y. Chen, B. H. Shao, J. Cheng and X. Li, Recent advances of small-molecule fluorescent probes for detecting biological hydrogen sulfide, *Front. Chem. Sci. Eng.*, 2022, **16**, 34–63.
- 10 X. Jia, W. Li, Z. H. Guo, Z. B. Guo, Y. Li, P. Z. Zhang, C. Wei and X. L. Li, An NBD-based mitochondrial targeting ratiometric fluorescent probe for hydrogen sulfide detection, *ChemistrySelect*, 2019, **4**, 8671–8675.
- 11 L. Zhou, G. Yuan and S. Hu, A 4-hydroxy-1,8-naphthalimide-based turn-on two-photon fluorescent probe for hydrogen polysulfide sensing, *J. Appl. Probab.*, 2020, **86**, 1071–1076.
- 12 Z. H. Zhang, S. Q. Li, Y. Z. Yan, J. B. Qu and J. Y. Wang, A novel fast-responsive fluorescent probe based on 1,3,5-triazine for endogenous H<sub>2</sub>S detection with large stokes shift and its application in cell imaging, *New J. Chem.*, 2021, **45**, 9756–9760.
- 13 Y. Y. Quan, L. L. Fan, H. Y. Shen, B. B. Wu, S. S. Kong, Y. S. Luo, Z. S. Huang and X. X. Ye, A multifunctional BODIPY based fluorescent probe for hydrogen sulfide detection and photodynamic anticancer therapy in HCT116 colon cancer cell, *Dyes Pigm.*, 2022, **197**, 109897.
- 14 S. Chen, P. Hou, J. W. Sun, H. J. Wang and L. Liu, Imidazo [1,5- $\alpha$ ]pyridine-based fluorescent probe with a large stokes shift for specific recognition of sulfite, *Spectrochim. Acta, Part A*, 2020, **225**, 117508.
- 15 P. Hou, J. W. Sun, H. J. Wang, L. Liu, L. W. Zou and S. Chen, TCF-imidazo[1,5- $\alpha$ ]pyridine: a potential robust ratiometric fluorescent probe for glutathione detection with high selectivity, *Sens. Actuators, B*, 2020, **304**, 127244.
- 16 P. Hou, S. Chen, G. L. Liang, H. M. Li and H. G. Zhang, A lysosome-targeted ratiometric fluorescent probe with a large blue shift for monitoring hypochlorous acid in living cells and zebrafish, *Spectrochim. Acta, Part A*, 2020, **229**, 117866.
- 17 P. Hou, S. Chen, G. L. Liang, H. M. Li and H. G. Zhang, Design of a facile fluorescent probe with a large stokes shift for hydrogen peroxide imaging *in vitro* and *in vivo*, *Spectrochim. Acta, Part A*, 2020, **236**, 118338.
- 18 S. Chen, P. Hou, J. W. Sun, H. J. Wang and L. Liu, A new long-wavelength emission fluorescent probe for imaging biothiols with remarkable stokes shift, *Spectrochim. Acta, Part A*, 2020, **241**, 118655.
- 19 M. W. Yang, J. L. Fan, J. J. Du and X. J. Peng, Small-molecule fluorescent probes for imaging gaseous signaling molecules: current progress and future implications, *Chem. Sci.*, 2020, **11**, 5127–5141.
- 20 Z. Y. Xu, T. Y. Qin, X. F. Zhou, L. Wang and B. Liu, Fluorescent probes with multiple channels for simultaneous detection of Cys, Hcy, GSH, and H<sub>2</sub>S, *Trends Anal. Chem.*, 2019, **121**, 115672.
- 21 H. N. Li, Y. X. Fang, J. J. Yan, X. Y. Ren, C. Zheng, B. Wu, S. Y. Wang, Z. L. Li, H. M. Hua, P. Wang and D. H. Li, Small-molecule fluorescent probes for H<sub>2</sub>S detection: advances and perspectives, *Trends Anal. Chem.*, 2021, **134**, 116117.
- 22 S. Muthusam, K. Rajalakshmi, D. W. Zhu, L. Zhao, S. Wang and W. Zhu, A novel lysosome targeted fluorophore for H<sub>2</sub>S sensing: enhancing the quantitative detection with successive reaction sites, *Sens. Actuators, B*, 2020, **320**, 128433.
- 23 W. Shu, S. Zang, C. Wang, M. Gao, J. Jing and X. Zhang, An endoplasmic reticulum targeted ratiometric fluorescent probe for sensing of hydrogen sulfide in living cells and zebrafish, *Anal. Chem.*, 2020, **92**, 9982–9988.
- 24 Y. Zhang, Y. Chen, Y. Bai, X. Xue, W. He and Z. Guo, FRET-based fluorescent ratiometric probes for the rapid detection of endogenous hydrogen sulphide in living cells, *Analyst*, 2020, **145**, 4233–4238.
- 25 P. Hou, J. Wang, S. Fu, L. Liu and S. Chen, Highly sensitive fluorescent probe based on a novel phenothiazine dye for

- detection of thiophenols in real water samples and living cells, *Anal. Bioanal. Chem.*, 2019, **411**, 935–942.
- 26 P. Hou, J. Wang, S. Fu, L. Liu and S. Chen, A new turn-on fluorescent probe with ultra-large fluorescence enhancement for detection of hydrogen polysulfides based on dual quenching strategy, *Spectrochim. Acta, Part A*, 2019, **213**, 342–346.
- 27 Y. Zheng, P. Hou, Y. Li, J. W. Sun, H. X. Cui, H. Y. Zhang and S. Chen, A phenothiazine-HPQ based fluorescent probe with a large stokes shift for sensing biothiols in living systems, *Molecules*, 2021, **26**, 2337–2349.
- 28 C. L. Shang, H. Y. Wang, T. J. Ni, K. W. Chang and C. P. Ge, A dicyanoisophorone-based near-infrared fluorescent probe with fast detection for H<sub>2</sub>S in living cells and zebrafish, *J. Lumin.*, 2022, **243**, 118669.
- 29 B. Yang, M. M. Su, Y. S. Xue, Z. X. He, C. Xu and H. L. Zhu, A selective fluorescence probe for H<sub>2</sub>S from biothiols with a significant regioselective turn-on response and its application for H<sub>2</sub>S detection in living cells and in living *Caenorhabditis elegans*, *Sens. Actuators, B*, 2018, **276**, 456–465.
- 30 L. Zhou, Z. Q. Cheng, N. Li, Y. X. Ge, H. X. Xie, K. Zhu, A. Zhou, J. Zhang, K. M. Wang and C. S. Jiang, A highly sensitive endoplasmic reticulum-targeting fluorescent probe for the imaging of endogenous H<sub>2</sub>S in live cells, *Spectrochim. Acta, Part A*, 2020, **240**, 118578.
- 31 Z. Q. Hu, A fluorescent probe based on tetrahydro[5]helicene derivative with large stokes shift for rapid and highly selective recognition of hydrogen sulfide, *Spectrochim. Acta, Part A*, 2019, **214**, 487–495.